

# Can lasers really refrigerate CdS nanobelts?

Yurii V. Morozov<sup>1,6</sup>, Shubin Zhang<sup>2,6</sup>, Anupam Pant<sup>3,6</sup>, Boldizsár Jankó<sup>2</sup>, Seth D. Melgaard<sup>4</sup>, Daniel A. Bender<sup>4\*</sup>, Peter J. Pauzauskie<sup>3,5\*</sup> & Masaru Kuno<sup>1,2\*</sup>

ARISING FROM Zhang, J. et al. *Nature* <https://www.nature.com/articles/nature11721> (2013)

Five years ago, Xiong and co-workers reported the net laser cooling of a CdS nanobelt<sup>1</sup>, which seemed to be the remarkable conclusion to a 16-year search for ways to successfully cool a semiconductor using light<sup>2,3</sup>. However, as we describe below, there are questions and concerns about this study that cast doubts on its validity.

Practical laser cooling of semiconductors remains an exciting goal, first and foremost because of the substantial cooling that is possible. Because band-edge carriers follow Fermi–Dirac statistics, temperatures as low as about 10 K are possible<sup>4</sup>. This is beyond the 50–100 K cooling floors achievable with rare-earth-doped glasses, where cooling is ultimately hampered by the Boltzmann population of rare-earth ions. Cryogenic semiconductor refrigerators, with cooling floors lower than those of existing Peltier coolers, would immediately find myriad uses in electronics and optoelectronics.

Although analogous optical cooling of gases has since been realized with great success<sup>5,6</sup>, condensed-phase optical cooling has progressed more slowly because of the considerable technical hurdles that have been encountered. So far, only rare-earth-doped materials have been verifiably cooled<sup>7–9</sup>. Laser cooling of semiconductors therefore remains a holy grail in the field of condensed-phase optical cooling.

Although there are no physical reasons why semiconductors may not be optically cooled<sup>4</sup>, realizing such cooling would be a monumental achievement because it would require materials with near-unity quantum yields—that is, materials effectively perfect from an optical standpoint. In this regard, any non-radiative relaxation pathway in the material will lead to heating. To highlight the precarious nature of optical cooling, non-radiative interband recombination, surface carrier trapping/relaxation and Auger recombination all lead to the conversion of nearly the entire semiconductor bandgap energy into heat. These heating pathways compete detrimentally with the energy of about  $k_B T$  ( $k_B$ , Boltzmann constant;  $T$ , surrounding temperature) extracted per photon per cycle of optical cooling.

The external radiative quantum efficiencies (EQEs) of semiconductors must consequently exceed about 97%, with the minimum EQE depending on the bandgap<sup>4</sup>. For GaAs, this means<sup>10</sup> that  $\text{EQE}_{\min} \geq 99\%$ . For CdS, the EQE requirement<sup>11</sup> is  $\text{EQE}_{\min} \geq 96.4\%$ . So far, the largest reported semiconductor EQE has been for a GaAs heterostructure, where  $\text{EQE} = 99.5\%$  was achieved after painstakingly maximizing the quality of its interfaces<sup>10</sup>. Even then, cooling was not realized. It is therefore remarkable that Xiong and co-workers<sup>1</sup> have observed laser cooling in vapour-grown CdS nanobelts using a synthesis with no particular emphasis on surface passivation or on maximizing overall EQEs.

Motivated by this unexpected success, a number of groups have tried to reproduce the seminal breakthrough of Xiong and colleagues. Until now, no one has succeeded in establishing CdS nanobelt optical cooling. This includes work done on nanobelts provided by the Xiong laboratory in Singapore, as well as with CdS nanobelts grown in the

USA following the reported synthetic protocols. Below we highlight the primary question that has arisen during these investigations.

The major issue encountered during these studies is an inconsistency in the reported cooling timescales. Namely, Xiong and co-workers show in figures 4b and 4e of their paper<sup>1</sup> that individual CdS nanobelts attached to and suspended over a pyramidal pit in a SiO<sub>2</sub>/Si substrate cool over the course of about 30 min. Figure 1a reproduces these data from an individual nanobelt excited at 532 nm. Most striking is that the observed cooling time is inconsistent with the characteristic timescale,  $\tau \approx \frac{C_p}{4 \left(\frac{A}{V}\right) \sigma T_o^3}$ , associated with the blackbody-limited cooling of a thermally isolated nanobelt. In this equation,  $C_p = 1.62 \times 10^6 \text{ J K}^{-1} \text{ m}^{-3}$  is the volumetric heat capacity of the nanobelt<sup>12</sup>;  $A$  (V) is its area (volume), assuming a length of  $L = 20 \mu\text{m}$ , a width of  $W = 5 \mu\text{m}$  and a thickness of  $H = 110 \text{ nm}$ ;  $\sigma$  is the Stefan–Boltzmann constant; and  $T_o = 300 \text{ K}$  is the surrounding temperature. What results is a cooling/heating timescale of  $\tau \approx 30 \text{ ms}$ , about four orders of magnitude faster than what has been reported.

Corroborating this, ref. <sup>13</sup> modelled heat dissipation and equilibration in an electromagnetically heated, singly clamped, rectangular CdS nanobelt of identical dimensions as above. Figure 1b illustrates the considered nanobelt system. The model shows that temperature equilibration occurs within 100  $\mu\text{s}$  (Fig. 1c). This is a discrepancy that exceeds the experimental values reported by Xiong and co-workers<sup>1</sup> by seven orders of magnitude. The discrepancy becomes even larger for calculations involving a doubly clamped nanobelt, where heat diffuses through both ends.

The existence of vastly longer cooling timescales could stem from the presence of an additional thermal load in the system. In practice, this would arise from the substrate on which the nanobelt rests. This scenario has been explored by Xiong and co-workers in ref. <sup>14</sup>, where they studied the direct cooling of a SiO<sub>2</sub>/Si substrate using a CdS nanobelt lying atop it. Curiously, nearly identical cooling timescales (about  $10^3 \text{ s}$ ) and temperatures were observed as those seen in the original study<sup>1</sup>.

Although the substrate thermal load could in principle explain the above-noted timescale discrepancy (Fig. 1), we note that neither ref. <sup>1</sup> nor ref. <sup>14</sup> considered heating effects in the Si substrate due to absorption of the incident 532-nm radiation. This is relevant because substrate heating will overwhelm any cooling induced by the nanobelt. Here a simple calculation (Si indirect bandgap, 1.12 eV; incident 532-nm radiation power, 6.3 mW; substrate reflectance of about 18% from a 300-nm SiO<sub>2</sub>/Si interface; nanobelt absorptance of about 5%) suggests that in the original study about 79% (about 5.0 mW) of the incident power will be absorbed by the substrate. This is over 50 times the reported nanobelt cooling power (97  $\mu\text{W}$ ).

A number of other questions and concerns arise upon careful analysis of the reported CdS nanobelt laser cooling. Xiong and co-workers have since reported laser cooling of other materials, such as hybrid

<sup>1</sup>Department of Chemistry and Biochemistry, University of Notre Dame, Notre Dame, IN, USA. <sup>2</sup>Department of Physics, University of Notre Dame, Notre Dame, IN, USA. <sup>3</sup>Department of Materials Science, University of Washington, Seattle, WA, USA. <sup>4</sup>Sandia National Laboratories, Albuquerque, NM, USA. <sup>5</sup>Pacific Northwest National Laboratory, Richland, WA, USA. <sup>6</sup>These authors contributed equally: Yurii V. Morozov, Shubin Zhang, Anupam Pant. \*e-mail: dabende@sandia.gov; peterpz@uw.edu; mkuno@nd.edu

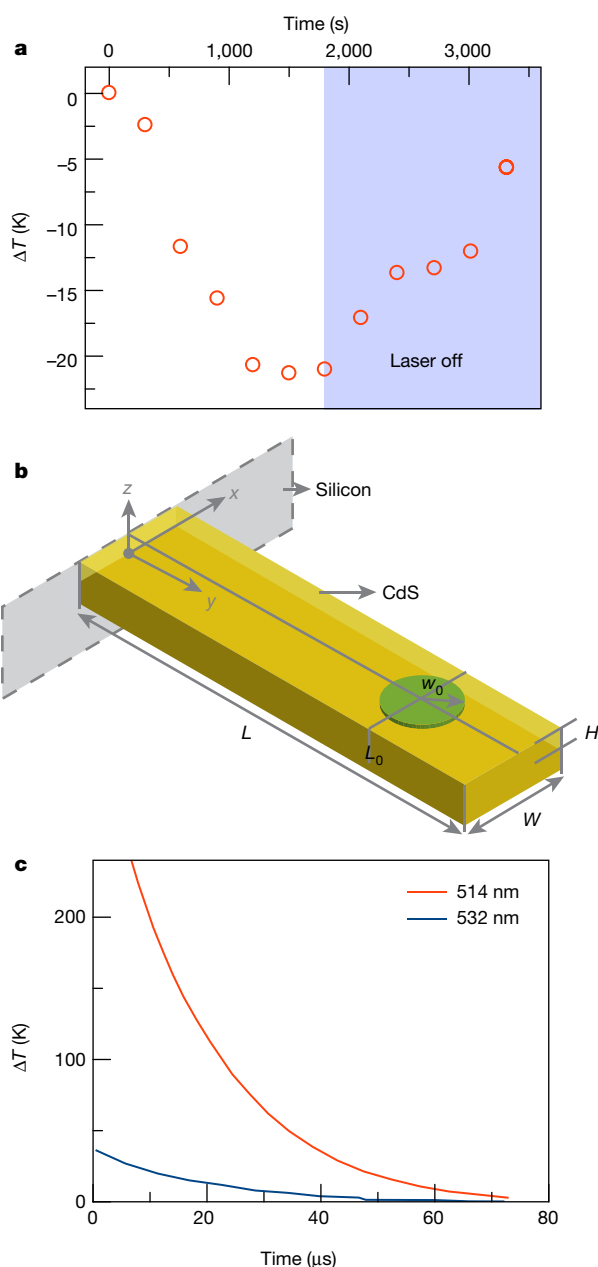


**Fig. 1 | Experimental and simulation results for CdS nanobelt laser cooling.** **a**, CdS nanobelt cooling and heating results reported in ref. <sup>1</sup>. **b**, Rectangular CdS nanobelt cantilever geometry used to model heat dissipation<sup>13</sup>. The laser spot is shown by the green circle. **c**, Resulting model cooling curves depicting the decay in the maximum steady-state temperature after the laser source (either 532 nm or 514 nm) has been switched off.

perovskites<sup>15</sup>. Although these results are equally intriguing as those of the original CdS nanobelt study, they too raise similar questions and concerns. On the basis of our results and analyses, we have serious doubts about the validity of claims made by Xiong and co-workers in

refs. <sup>1,14,15</sup>. We therefore suggest that it is too early to conclude whether laser cooling of semiconductors has truly been achieved.

## Data availability

All data are available from the corresponding authors upon reasonable request.

Received: 25 April 2018; Accepted: 25 March 2019;

Published online 26 June 2019.

1. Zhang, J., Li, D., Chen, R. & Xiong, Q. Laser cooling of a semiconductor by 40 kelvin. *Nature* **493**, 504–508 (2013).
2. Gauck, H., Gfroerer, T. H., Renn, M. J., Cornell, E. A. & Bertness, K. A. External radiative quantum efficiency of 96% from a GaAs/GaN heterostructure. *Appl. Phys. A* **64**, 143–147 (1997).
3. Sheik-Bahae, M. & Epstein, R. I. Optical refrigeration. *Nat. Photon.* **1**, 693–699 (2007).
4. Sheik-Bahae, M. & Epstein, R. I. Can laser light cool semiconductors? *Phys. Rev. Lett.* **92**, 247403 (2004).
5. Hänsch, T. W. & Schawlow, A. L. Cooling of gases by laser radiation. *Opt. Commun.* **13**, 68–69 (1975).
6. Chu, S. Laser manipulation of atoms and particles. *Science* **253**, 861–866 (1991).
7. Epstein, R. I., Buchwald, M. I., Edwards, B. C., Gosnell, T. R. & Mungan, C. E. Observation of laser-induced fluorescent cooling of a solid. *Nature* **377**, 500–503 (1995).
8. Melgaard, S. D., Albrecht, A. R., Hehlen, M. P. & Sheik-Bahae, M. Solid-state optical refrigeration to sub-100 Kelvin regime. *Sci. Rep.* **6**, 20380 (2016).
9. Roder, P. B., Smith, B. E., Zhou, X., Crane, M. J. & Pauzauskie, P. J. Laser refrigeration of hydrothermal nanocrystals in physiological media. *Proc. Natl Acad. Sci. USA* **112**, 15024–15029 (2015).
10. Bender, D. A., Cederberg, J. G., Wang, C. & Sheik-Bahae, M. Development of high quantum efficiency GaAs/GaN double heterostructures for laser cooling. *Appl. Phys. Lett.* **102**, 252102 (2013).
11. Morozov, Y. V. et al. Defect-mediated CdS nanobelt photoluminescence up-conversion. *J. Phys. Chem. C* **121**, 16607–16616 (2017).
12. Madelung O., Rössler U. & Schulz M. (eds) in *II-VI and I-VII Compounds; Semimagnetic Compounds* Vol. 41B 1–3 (Springer, 1999).
13. Pant, A. et al. Optomechanical thermometry of nanoribbon cantilevers. *J. Phys. Chem. C* **122**, 7525–7532 (2018).
14. Li, D., Zhang, J., Wang, X., Huang, B. & Xiong, Q. Solid-state semiconductor optical cryocooler based on CdS nanobelts. *Nano Lett.* **14**, 4724–4728 (2014).
15. Ha, S.-T., Shen, C., Zhang, J. & Xiong, Q. Laser cooling of organic–inorganic lead halide perovskites. *Nat. Photon.* **10**, 115–121 (2016).

**Acknowledgements** Sandia National Laboratories is a multi-mission laboratory managed and operated by National Technology and Engineering Solutions of Sandia, LLC., a wholly owned subsidiary of Honeywell International, Inc., for the US Department of Energy's National Nuclear Security Administration under contract DE-NA0003525. The Pacific Northwest National Laboratory is a multiprogramme national laboratory operated for the US Department of Energy by Battelle under contract number DE-AC05-76RL01830. Y.V.M., S.Z., A.P., P.J.P. and M.K. acknowledge financial support from the MURI:MARBLE project under the auspices of the Air Force Office of Scientific Research (award number FA9550-16-1-0362).

**Author contributions** Y.V.M., S.Z., B.J., S.D.M., D.A.B., P.J.P. and M.K. analysed the original study. M.K., Y.V.M., J.B., A.P. and P.J.P. wrote the manuscript. All authors discussed the results and contributed to the final manuscript.

**Competing interests** The authors declare no competing interests.

## Additional information

**Reprints and permissions information** is available at <http://www.nature.com/reprints>.

**Correspondence and requests for materials** should be addressed to D.A.B., P.J.P. or M.K.

**Publisher's note:** Springer Nature remains neutral with regard to jurisdictional claims in published maps and institutional affiliations.

© The Author(s), under exclusive licence to Springer Nature Limited 2019

# Reply to: Can lasers really refrigerate CdS nanobelts?

Jun Zhang<sup>1</sup>, Dehui Li<sup>2</sup> & Qihua Xiong<sup>3\*</sup>

REPLYING TO Y. V. Morozov et al. *Nature* <https://doi.org/10.1038/s41586-019-1269-1> (2019)

In the accompanying comment<sup>1</sup>, Morozov et al. questioned the validity of laser cooling of semiconductors in CdS nanobelts and other subsequent demonstrations by our group<sup>2–4</sup>. Their main argument is the large discrepancy between our experimental observations and their simulation, which is based on a COMSOL heat-transfer model<sup>5</sup>, concerning the time required to reach equilibrium. In the following, we explain that their arguments are not sufficient to support their conclusions.

The computational model established by Pant et al.<sup>5</sup> does not capture the thermal contact conductivity between two dissimilar interfaces<sup>6</sup>. The thermal couplings among the CdS nanobelt, the silicon substrate and the copper heat sink determine the overall cooling response time. In ref. <sup>3</sup>, we considered the two thermal contact conductivities in our model. We used the time response of the warming-up process to deduce the value of the thermal contact conductivity, which was then used to simulate the cooling process in comparison with our experimental observation (figure 3b in ref. <sup>3</sup>). The other limitation of the model of Pant et al. is that they did not consider blackbody radiation. With maximum heating as high as 1,494 K, thermal radiation inevitably becomes a most important channel to dissipate heat, and the sample should be decomposed.

Here we use modelling to provide further insight into the cooling response time, by considering the thermal contact conductivities between the nanoribbon and the silicon-on-insulator (SOI) substrate ( $G_1$ ) and between the SOI substrate and the heat sink ( $G_2$ ) (Fig. 1, Methods). Three probes are used to monitor the transient temperature variation during the simulation: Probe 1, at the middle point of the nanoribbon; Probe 2, inside the nanoribbon, slightly above the contact; and Probe 3, at the centre of the SOI substrate. When the thermal contact conductivity  $G_1$  is  $1.0 \times 10^7 \text{ W m}^{-2} \text{ K}^{-1}$ , the results for different  $G_2$  values are as shown in Fig. 1b. Figure 1c displays the response time when  $G_2$  is  $1.0 \times 10^6 \text{ W m}^{-2} \text{ K}^{-1}$  and  $G_1$  varies from  $10^5 \text{ W m}^{-2} \text{ K}^{-1}$  to  $10^9 \text{ W m}^{-2} \text{ K}^{-1}$ .

It can be seen from Fig. 1b that the thermal contact conductivity  $G_2$  has an important role in determining the overall response time. The response time also depends on the location. In the nanoribbon far from the contact, the response time decreases sharply when  $G_2$  increases, whereas in the SOI substrate and the region just above the contact, the response time is much longer. Those observations indicate that the coupling with the heat sink is important in determining the thermal response of the nanoribbon.

The response time of the probes in the nanoribbon can also be affected by  $G_1$ , that is, the coupling between the nanoribbon and the SOI substrate, as can be seen from Fig. 1c. For the region above the contact, the response times are much longer when the coupling between the nanoribbon and the substrate is strong. With different coupling strengths, the response time of Probe 2 can vary from tens of microseconds to about ten seconds. According to the simulation results, the temperature distribution inside the SOI substrate is quite

uniform. Considering that the heat capacity of the nanoribbon is much smaller than that of the SOI substrate, we can estimate the average temperature of the substrate and nanoribbon (the nanoribbon temperature is only slightly different from that of the substrate when  $G_1 = 1.0 \times 10^7 \text{ W m}^{-2} \text{ K}^{-1}$ , as can be seen in the previous work<sup>3</sup>).

Our modelling results further suggest that a long cooling response time could result from the combination of a strong thermal coupling between the nanoribbon and the substrate and a much weaker coupling between the silicon wafer and the copper heat sink. Thermal contact conductivity depends strongly on the contact quality, the pressure and the materials on both sides. It is possible to have a high thermal contact conductivity of about  $10^7$ – $10^8 \text{ W m}^{-2} \text{ K}^{-1}$ , especially for micrometre-sized flexible samples—for example, the thermal contact conductivity between manually transferred graphene and silicon oxide can reach<sup>7</sup> about  $8.3 \times 10^7$ – $1.8 \times 10^8 \text{ W m}^{-2} \text{ K}^{-1}$ . A thermal contact conductivity of about  $25 \text{ MW m}^{-2} \text{ K}^{-1}$  has been reported for a sandwiched Au/Ti/graphene/SiO<sub>2</sub> interface<sup>8</sup>. Concerning the thermal contact conductivity between a silicon wafer and a copper heat sink, we have not found any measurements on such dissimilar interfaces. Nonetheless, some previous studies may help to shed light on this issue. For instance, Lee et al. measured the thermal contact resistance of an Al–Al interface and found it to be 5–6 orders of magnitude lower than that of the bulk<sup>9</sup>. Using their parameters, we estimated a thermal contact conductivity of about  $0.2$ – $2.0 \text{ kW m}^{-2} \text{ K}^{-1}$ . Another paper<sup>10</sup> reported a thermal contact conductivity of about  $10 \text{ kW m}^{-2} \text{ K}^{-1}$  under a pressure of about 3 MPa. For the dissimilar-material interface between a silicon wafer and copper without pressure, one would expect an even lower thermal contact conductivity—for example, the same paper<sup>10</sup> reported a total thermal conductivity of about  $1.16 \text{ kW m}^{-2} \text{ K}^{-1}$  for the bolted assembly Al/RTV/Al, where RTV denotes a layer of room-temperature vulcanizing silicone rubber of about 0.2 mm.

Regarding the criteria for sample selection for laser cooling, we select samples with the following properties<sup>2,3</sup>: (1) strong phonon-assisted anti-Stokes photoluminescence with a linear laser power dependence; (2) absence of sub-gap defect emission, as shown in Fig. 2; (3) high external quantum efficiency. As shown in refs <sup>5,11</sup>: (i) there is a broad defect emission in the range 560–800 nm, which is often observed in bulk crystal or nanobelts when the synthesis condition is sub-optimal<sup>12,13</sup>; (ii) the exponent of the integrated intensity versus the excitation power is 1.34, which indicates a considerable contribution from up-conversion induced by two-photon absorption; (iii) there are low external quantum efficiencies of 10%–64%. As Morozov et al. discussed in their original paper<sup>11</sup>, those defects are the primary sources of degradation for the external quantum efficiency. For the nanobelt that they chose from the samples that we provided, the emission also shows defect emission and low quantum efficiency. It is possible that the CdS nanobelts have degraded during transportation, or with time.

<sup>1</sup>State Key Laboratory of Superlattices and Microstructures, Institute of Semiconductors, Chinese Academy of Science, Beijing, China. <sup>2</sup>School of Optical and Electronic Information, Huazhong University of Science and Technology, Wuhan, China. <sup>3</sup>Division of Physics and Applied Physics, School of Physical and Mathematical Sciences, Nanyang Technological University, Singapore, Singapore. \*e-mail: Qihua@ntu.edu.sg

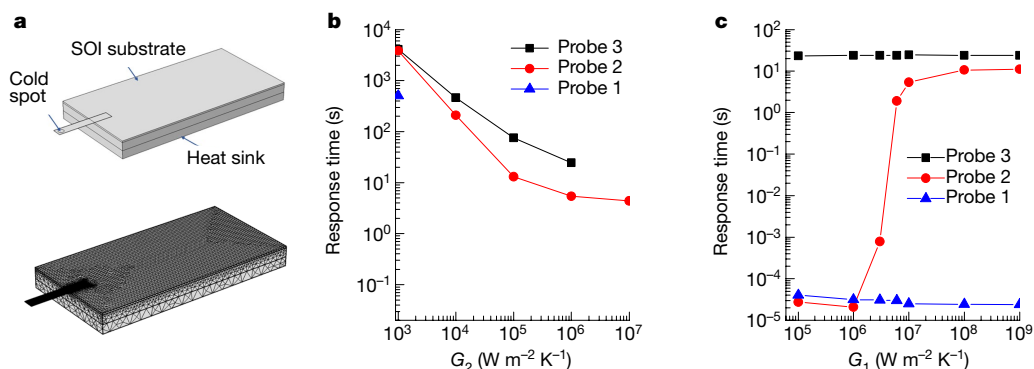


**Fig. 1 | Simulation of cooling response times.** **a**, The simulation setup (top) and the mesh used for the simulation (bottom). **b**, Response times of the probed points for different interfacial conductivities  $G_2$  when

$G_1 = 1.0 \times 10^7 \text{ W m}^{-2} \text{ K}^{-1}$ . **c**, Response times of the probed points for different contact conductivities  $G_1$  when  $G_2 = 1.0 \times 10^6 \text{ W m}^{-2} \text{ K}^{-1}$ .

Concerning the parasitic absorption due to silicon, we argue that this absorption is not a major issue for local-temperature thermometry for the following reasons: (1) beyond the confocal point, the laser is rather diffusive and diverged—therefore, the heat flux due to absorption is small; (2) the large thermal conductivity (about  $148 \text{ W m}^{-2} \text{ K}^{-1}$ ) of silicon, which indicates considerable heat dissipation power from the silicon to the copper heat sink (via the silicon–copper thermal contact surface). We agree that in our current simulation model, it is not possible to provide a quantitative assessment of parasitic absorption. Nonetheless, it is clear that the anti-Stokes excitation did not introduce any noticeable local temperature increase, judging from the Stokes/anti-Stokes ratio of the Raman signal due to Si transverse optical phonons. One hypothesis is that the heat flow in the far field can be readily dumped to the heat sink owing to the large thermal conductivity of silicon.

Last but not least, the arguments of Morozov et al.<sup>1</sup> are mainly based on Pant et al.<sup>5</sup> and Morozov et al.<sup>11</sup>, which reported self-contradictory results. As shown in their table 1, Pant et al.<sup>5</sup> reported an internal temperature increase  $\Delta T_{\text{ms}}$  (increase at the hottest point, that is, the maximum steady-state temperature  $\Delta T_{\text{max}}$ ) of 371 K (1,494 K) by a 532-nm laser (1.8 mW power, roughly  $43.3 \text{ kW cm}^{-2}$  power density) (both values are relative to ambient temperature). This value is unreasonably high and it contradicts the Morozov et al.<sup>11</sup> measurements, in which heating of about 5 K was observed in CdS nanobelts excited by a 480-nm laser with a power density of  $1,200 \text{ kW cm}^{-2}$  (see supplementary figure 16 in ref.<sup>9</sup>). The absorption coefficients of the CdS nanobelts are about  $3 \times 10^4 \text{ cm}^{-1}$  and  $8 \times 10^5 \text{ cm}^{-1}$  at 532 nm and 480 nm, respectively<sup>2,14</sup>.

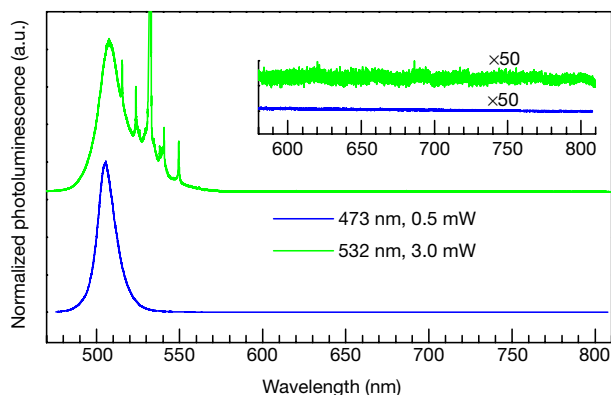


**Fig. 2 | Photoluminescence spectra.** Typical Stokes and anti-Stokes photoluminescence spectra of CdS nanobelts selected for laser-cooling testing in ref.<sup>2</sup>. a.u., arbitrary units.

Following the model of Pant et al.<sup>5</sup>, we can estimate that the heating should be around  $2.7 \times 10^5 \text{ K}$  when CdS is excited by the excitation condition reported in ref.<sup>11</sup>; this is 4–5 orders of magnitude higher than the measured value<sup>11</sup>.

## Methods

We build a model similar to that reported in ref.<sup>5</sup> (Fig. 1a), considering the thermal contact conductivities between the nanoribbon and the SOI substrate ( $G_1$ ) and between the SOI substrate and the heat sink ( $G_2$ ). Convection and radiation heat transfer are neglected. A constant heat flow of  $70 \mu\text{W}$  is applied at the cold spot. The bottom surface of the copper heat sink (1 cm thick) is set at 300 K. Other parameters such as the thermal conductivities of Si,  $\text{SiO}_2$  and CdS have the same values as those used in previous work<sup>3</sup>. To reduce the computational cost, the substrate size is shrunk to  $50 \times 50 \mu\text{m}^2$  from the original value of about  $1 \times 1 \text{ cm}^2$  and the specific heat of the substrate is scaled accordingly to maintain the same total heat capacity. The thermal contact conductivity  $G_2$  is also scaled accordingly with a factor of  $5 \times 10^4$ . The response time is taken as 67% of the total time required to reach thermal equilibrium.

## Data availability

All data are available from the corresponding author(s) upon reasonable request.

- Morozov, Y. V. et al. Can lasers really refrigerate CdS nanobelts? *Nature* <https://doi.org/10.1038/s41586-019-1269-1> (2019).
- Zhang, J. et al. Laser cooling of a semiconductor by 40 kelvin. *Nature* **493**, 504–508 (2013).
- Li, D. H. et al. Solid-state semiconductor optical cryocooler based on CdS nanobelts. *Nano Lett.* **14**, 4724–4728 (2014).
- Ha, S. T. et al. Laser cooling of organic–inorganic lead halide perovskites. *Nat. Photon.* **10**, 115–121 (2016).
- Pant, A. et al. Optomechanical thermometry of nanoribbon cantilevers. *J. Phys. Chem. C* **122**, 7525–7532 (2018).
- Swartz, E. T. & Pohl, R. O. Thermal boundary resistance. *Rev. Mod. Phys.* **61**, 605–668 (1989).
- Chen, Z. et al. Thermal contact resistance between graphene and silicon dioxide. *Appl. Phys. Lett.* **95**, 161910 (2009).
- Koh, Y. K. et al. Heat conduction across monolayer and few-layer graphenes. *Nano Lett.* **10**, 4363–4368 (2010).
- Lee, S. Y. et al. Measurement of interface thermal resistance with neutron diffraction. *J. Heat Transfer* **136**, 031302 (2014).
- Yeh, C. L. et al. An experimental investigation of thermal contact conductance across bolted joints. *Exp. Therm. Fluid Sci.* **25**, 349–357 (2001).
- Morozov, Y. V. et al. Defect-mediated CdS nanobelt photoluminescence up-conversion. *J. Phys. Chem. C* **121**, 16607–16616 (2017).
- Wang, C. et al. Structure control of CdS nanobelts and their luminescence properties. *J. Appl. Phys.* **97**, 054303 (2005).
- Du, K. Z. et al. CdS bulk crystal growth by optical floating zone method: strong photoluminescence upconversion and minimum trapped state emission. *Opt. Eng.* **56**, 011109 (2016).
- Rossler, U. (ed.) *Landolt-Bornstein Numerical Data and Functional Relationships in Science and Technology – New Series III* (Springer, 1999).

**Acknowledgements** We thank B. Huang from the Hong Kong University of Science and Technology for constructive discussions and help with the thermal analysis and modelling.

**Author contributions** J.Z. and D.L. further analysed previous data and conducted the simulation. All authors prepared and wrote this reply.

**Competing interests** The authors declare no competing interests.

## Additional information

**Reprints and permissions information** is available at <http://www.nature.com/reprints>.

**Correspondence and requests for materials** should be addressed to Q.X.

**Publisher's note:** Springer Nature remains neutral with regard to jurisdictional claims in published maps and institutional affiliations.

© The Author(s), under exclusive licence to Springer Nature Limited 2019